On the trade-off between timeliness and accuracy for low voltage distribution system grid monitoring utilizing smart meter data

Kemal, Mohammed Seifu; Martin-Loeches, Ruben Sanchez; Olsen, Rasmus Løvenstein; Iov, Florin; Schwefel, Hans-Peter Christian

Published in:
International Journal of Electrical Power and Energy Systems

DOI (link to publication from Publisher):
10.1016/j.ijepes.2020.106090

Publication date:
2020

Document Version
Publisher's PDF, also known as Version of record

Electrical Power and Energy Systems 121 (2020) 106090

Contents lists available at ScienceDirect

Electrical Power and Energy Systems

journal homepage: www.elsevier.com/locate/ijepes

On the trade-off between timeliness and accuracy for low voltage distribution system grid monitoring utilizing smart meter data

Mohammed Kemal[a], Ruben Sanchez[b], Rasmus Olsen[a], Florin Iov[b], Hans-Peter Schwefel[a,c]

[a] Department of Electronic Systems, Aalborg University, Aalborg, Denmark
[b] Department of Energy and Technology, Aalborg University, Aalborg, Denmark
[c] GridData GmbH, Anger/Traunstein, Germany

ARTICLE INFO

Keywords:
Smart grid
AMI
Real-time
Monitoring
Adaptive data collection
Low voltage grid
Distribution system
State estimation

ABSTRACT

Due to limited bandwidth and high delays in access to Smart Meter measurements, it is not possible in most cases to access measurements from the complete set of smart meters in a low-voltage grid area for distribution grid monitoring. Distribution system state estimation can be performed based on measurements of voltage and active and reactive power from a subset of selected smart meters. Increasing the number of selected smart meters will, on the one hand, increase the accuracy of distribution system state estimation, while on the other hand, it will degrade timeliness of the monitoring data. This paper proposes to utilize part of the idle time of the legacy periodic smart meter data collection for access to measurements from the subset of selected smart meters for distribution system state estimation. It subsequently proposes a methodology on how to quantitatively analyze this trade-off. The methodology is applied to an example LV grid area with 20 customers using a weighted least square state estimation with support of pseudo-measurements obtained during the regular smart meter collection cycle.

1. Introduction

In recent years, the electrical behavior of Low Voltage (LV) grids has been transforming due to the increasing penetration of Distributed Energy Resources [1]. Traditionally, the generation of power required to feed the loads of the entire electrical grid was centralized in large power plants placed at the High Voltage (HV) level where the LV grids were merely seen as loads. However, this operational philosophy is changing due to the appearance of Decentralized or Distributed Generation based on Renewable Energy Sources such as Photo Voltaic (PV) panels or small scale wind turbines. Additionally, a new type of loads such as single-phase connected heat pumps, electric boilers or electrical vehicles produce voltage and power profiles never seen before at the LV level. However, these new loads and DGs can cause technical challenges, such as sudden voltage dips and swells, unexpected and uncontrollable voltage variations, congestion or bidirectional power flows [2].

1.1. Background and problem scope

In this context, Distribution System Operators (DSOs) lack the technologies required to ensure that the grid fulfills operational requirements defined by grid codes and technical standards [3]. As prerequisite of assuring operational requirements, the DSOs require as a first step a reliable source of information about the operational grid state. In electricity grids, the state of the grid can be fully captured by the complex voltage phasors in every node of the system [4]. The deployment of Phasor Measurement Units (PMUs) would provide such voltage phasors, but the high clock synchronisation needs in most cases make the deployment too costly and hence infeasible for low-voltage grids. On the other hand, there is an undergoing deployment of Smart Meters (SMs) at the LV level which is close to 100% in some countries. However, the raw measurements from the devices cannot be directly considered since they contain noise due to different sources, e.g. measurement class, gross errors, etc. [4], and they do not provide phase angle information across different measurement points. Additionally, it might not be economically feasible to acquire measurements from every device. Therefore, the state of the power grid needs to be calculated from an incomplete number of potentially erroneous measurements, called state estimation.

1.2. System architecture and scope

Modern Advanced Metering Infrastructure (AMI) encompasses SMs,

E-mail addresses: seifu@es.aau.dk (M. Kemal), rsm@et.aau.dk (R. Sanchez), rlo@es.aau.dk (R. Olsen), fi@et.aau.dk (F. Iov), hps@es.aau.dk (H.-P. Schwefel).
URLs: http://kom.aau.dk/~rlo/ (R. Olsen), http://personprofil.aau.dk/104288?lang=en (F. Iov).

https://doi.org/10.1016/j.ijepes.2020.106090
Received 17 May 2019; Received in revised form 4 April 2020; Accepted 6 April 2020
Available online 29 April 2020

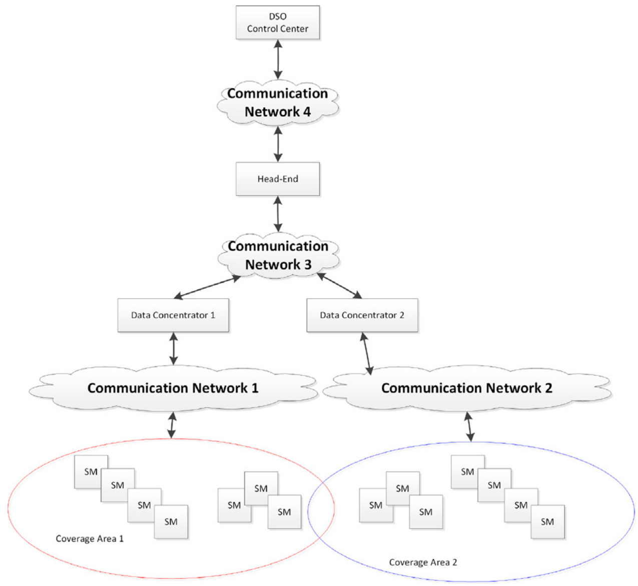

Fig. 1. AMI system architecture [5].

data concentrators (DC) and central system units defining a new AMI architecture. Fig. 1 illustrates a simplified high-level structure of AMI used in LV distribution grids. SMs connect to so-called concentrators by different communication technologies such as cellular, PLC, or wireless mesh. From the DC the collected information is pushed to the head end system (HES) from where information is made available to other components located at DSO control centers via a dedicated interface.

Often the networks used to collect data (Communication Network 1 and 2 in Fig. 1) are based on a technology that offers a huge penetration rate, because information from meters currently are used for billing only. Hence, the requirements of connectivity is 100% which previously has been hard to achieve, and with the requirements of data collection frequency of a month, timing requirements have been quite relaxed, hence these networks are currently not directly able to support a high data transport capacity. Communication Networks 3 and 4 are often modern technologies as 3G, 4G, Fiber or any other type of fast, high capacity backbone networks, with sufficient bandwidth for high volume data transmissions. The capacity constraint in the communication between SM and DC leads to long cycles of access to meter data (6–24 h.) making the readings hard to use directly for any smart grid solutions.

1.3. Contribution and paper structure

This paper proposes an approach to extend existing Smart Meter data access schemes by dedicated requests to voltage measurements of a subset of selected smart meters. The paper analyzes the trade-off that results from increasing the number of selected smart meters for dedicated measurement access: the more Smart Meters are used, the smaller the error of the state estimator while at the same time the timeliness of the grid state becomes worse. This trade-off is quantitatively characterized for an example of a realistic Low-Voltage grid with low-bandwidth access to Smart Meters when applying the known method of weighted least squares (WLS) state estimation.

The main contributions of the paper can be summarized as follows (i) monitoring of LV grids is approached combining ICT and electrical aspects, (ii) propose concepts for embedding periodic data collection for state estimation in idle periods of legacy smart metering systems. (iii) Investigate the use of WLS-based distribution system state estimation for LV grid monitoring with a focus on the cumulative impact of the number of selected SMs on monitoring system accuracy and its timeliness. (iv) Provide an outlook on how the presented approaches facilitate future research directions to support near real-time monitoring of LV distribution grids.

Section 2 presents related work and positions the contributions in this paper. In Section 3, the system context and the general approach for embedding access to selected Smart Meter data for state estimation in legacy systems are introduced. Section 4 analyzes the timeliness of the accessed data as resulting from such access to selected SMs. Section 5 introduces the approach for distribution system state estimation, the assessment scenario and the results for the state estimation accuracy. The results of the quantitative analysis characterize the trade-off between timeliness and state estimation accuracy in Section 6. Finally, this work is concluded in Section 7 and an outlook on how to support near real-time monitoring of LV grids is provided.

2. Related work

State estimation was first applied to HV power systems in the 70s [6]. It increased the operational capabilities of system operators enabling to establish energy management systems equipped with an online state estimation [7] among other functions. Nonetheless, until the deployment of SMs started to take place, there were no telemetered measurements available in the LV grids, and thus, state estimation techniques could not be implemented.

Weighted Least Square (WLS) is the most widely used and investigated technique for state estimation, specially applied to the monitoring of high and medium voltage grids. As detailed in [8] its application to LV grids is not straightforward; main challenges are increased computational requirements, accentuated numerical instability issues, and the low bandwidth of actual metering systems. Of special interest for this paper are the constraints related to the communication infrastructures deployed for the data acquisition in LV grids, see Fig. 1. Researchers have been working on the design of the Distribution System State Estimation (DSSE), as many advanced technologies are being implemented in distribution systems. Baran and Kelly suggested a DSSE methodology for real-time control of the distribution system based on the WLS approach and used a three-phase node voltage formulation [9]. The latest tree-based DSSE was proposed in [10,11]. Likewise, different methods have been proposed to solve DSSEs for unbalanced and/or asymmetrical systems [10,12,13] and radial networks [14]. However, the introduction of meshed topologies in future smart distribution networks renders some of these methods inapplicable. Admittance matrix based methods are introduced in [15] and improved in [16]. Therion et al. proposed a DSSE that would unify power flow and short-circuit calculation algorithms to achieve a unified DSSE with desirable numerical characteristics using modified augmented matrices [16].

A DSSE solution on the basis of synchronized measurements is built in [17]. Reference [10] shows that SMs can improve the accuracy of the DSSE, provided that SM measurements are relatively synchronized. Furthermore, treating signals as if they were all synchronized measurements may reduce the quality of DSSE, as the time difference between measurements may be substantial in practice. In order to take this latency into account, the precision of the available SM measurements can be decreased. For example, Wu et al. [18] believed that the available smart meter measurements had two error rates (2 per cent or 10 per cent), while Junqi et al. [19] considered that all smart meter measurements had the same error (10 per cent). However, approaches [18,19] do not take into account historical patterns of short-term load variability and the duration of time that has elapsed between the measurement sampling and the DSSE execution. Alternative approaches involve modeling loads using a neural network for DSSE applications [19]. The issue with this method is that training requires a reliable year-round load flow analysis that is not available without a reliable DSSE.

In power systems, the estimated states will be updated in a periodic fashion, event-triggered strategy or a mixture of both [20,21]. Of course, the followed strategy depends on the technological constraints of measurement devices and communication infrastructures. For instance, in HV grids, the Supervisory Control and Data Acquisition (SCADA) system monitors states using measurements gathered every few seconds [22]. Using Phasor Measurement Units allows tracking the dynamic behavior of the system due to measurement synchronization and faster reading updates [21].

The inclusion of measurement errors in calculation of electrical parameters in distribution grids has been addressed in [23]: the paper presents an approach to derive confidence intervals on the calculated electrical parameters, assuming normally distributed measurement errors. The paper studies the confidence intervals of the resulting calculations of feeder currents, when decreasing the number of available measurements and replacing them by pseudo-measurements with high variance.

Ideally, implementing monitoring systems for LV grids in near real-time would require to acquire information from every SM placed along the grid to reconstruct an accurate view of the operating scenario. However, the number of SMs (and thus, the number of electrical nodes) in LV grids might rise up to thousands, limited by communication technologies leading to slow update rates [8]. In order to relax the AMI performance requirements, smart metering data can be in some cases substituted by so-called pseudo-measurements which are artificially created measurements based on historical smart metering readings [24]. In case of SM failure or communication network bandwidth constraints, pseudo-measurements are of utmost importance in LV grids to ensure grid observability, which is defined by the SE capability to provide accurate estimates of the entire system given the input measurements. Grid observability depends on the number and position within the grid of available measurements [4].

The novelty of our work in comparison to the above is the assessment of the trade-off between accuracy and timeliness for DSSE based on periodical data collection utilizing idle periods of legacy smart meter systems.

The architecture in Fig. 1 is a logical view of the AMI network, but it also applies to the representation of a physical view defined by the type of communication technology used and geographical representation. There exist many realizations of the communication networks in Fig. 1.

The primary constraint for data collection is at CN1 and CN2 due to the low bandwidth technologies deployed between SM and concentrators. Communication technologies and related Quality of Service (QoS) characteristics are thus of paramount importance for LV distribution grid monitoring using AMI systems with a real-time, reliable and efficient bi-directional data flow. Since there are a considerable amount of customers/prosumers located in a LV grid, and thus, a large number of potential measurement points, deploying and maintaining traditional wired communication, e.g., Ethernet or Fiber would not be economically feasible for grid operators. Therefore, deployment of widely available existing communication technologies such as wireless cellular, e.g., 2G, 3G and radio mesh networks or PLC present a cost-effective solution for the AMI system. However, this comes at the cost of small data rate, and imperfect/changing QoS properties within the network [25]. For instance, narrowband PLC has data-rate ranging from 10 to 500 Kbps [26].

3. System description

In this section we describe the detailed behavior of the AMI system and the embedding of smart meter data access for state estimation in the AMI legacy behavior.

The architecture in Fig. 1 is a logical view of the AMI network, but it also applies to the representation of a physical view defined by the type of communication technology used and geographical representation. There exist many realizations of the communication networks in Fig. 1.

The primary constraint for data collection is at CN1 and CN2 due to the low bandwidth technologies deployed between SM and concentrators. Communication technologies and related Quality of Service (QoS) characteristics are thus of paramount importance for LV distribution grid monitoring using AMI systems with a real-time, reliable and efficient bi-directional data flow. Since there are a considerable amount of customers/prosumers located in a LV grid, and thus, a large number of potential measurement points, deploying and maintaining traditional wired communication, e.g., Ethernet or Fiber would not be economically feasible for grid operators. Therefore, deployment of widely available existing communication technologies such as wireless cellular, e.g., 2G, 3G and radio mesh networks or PLC present a cost-effective solution for the AMI system. However, this comes at the cost of small data rate, and imperfect/changing QoS properties within the network [25]. For instance, narrowband PLC has data-rate ranging from 10 to 500 Kbps [26].

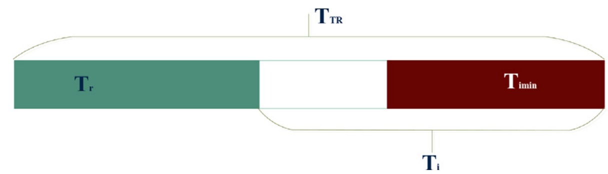

Fig. 2. AMI reading cycle.

3.1. Standard AMI data access

The low bandwidth AMI Communication networks result in a very slow update of data and long delays which affect the quality of information to support near real-time low voltage grid monitoring. Fig. 2 shows a typical AMI reading cycle where a concentrator repeats the pulling of data from all meters periodically with a period of total reading time (T_{TR}). For example, a typical reading cycle could be 6 h or once or twice a day. The DC pulls the SM measurements from all the SMs in its range, which results in reading time T_r. The value for T_r depends on the number of SMs and the round-trip communication delays between SM and DC. The required T_r must be executed every cycle by the AMI system to collect the mandatory data for billing of customer consumption. The idle time T_i is the remaining time from the fixed total allocated reading time of T_{TR} ($T_{TR} = T_r + T_i$) [27]. The idle time has a lower bound, minimum idle time T_{imin}, as there are some system services such as software updates that need to be performed during the idle time. The remaining idle time (T_i - T_{imin}) can potentially be used for reading selected relevant SMs for support of DSSE. The approach in this paper is to utilize the spare idle time to provide measurements to be used by DSSE.

In comparison with other voltage levels in the power system, LV grids are highly unobservable due to the low ratio between available measurements and system states. Nonetheless, pseudo-measurements are less accurate than SM measurements impacting the performance of the DSSE [28]. Thus there exist a trade-off between the capacity of the AMI system to provide relevant measurements and the DSSE performance measured by the accuracy of the estimates states. The capacity of AMI data access system to provide relevant measurements for monitoring is constrained by the spare idle time presented above. The more SM measurements are supplied during the spare idle time; the less the SE utilizes pseudo-measurements and the higher the accuracy. The relationship and trade-off between the capacity of AMI to provide relevant SM information and accuracy of DSSE is further analyzed in detail in the paper.

3.2. Snapshot measurements of selected Smart Meters for LV DSSE

The spare idle time has a limited capacity to collect relevant SM to be used by the DSSE. The relevant SM IDs accessed for this purpose are collected in vector of size R, and the time it takes to collect them is referred as timeliness (Δt_R) which is shown in Fig. 3. Here the assumption is that these R Smart Meters measure electrical parameters continuously every second and store it in a buffer (respectively over a

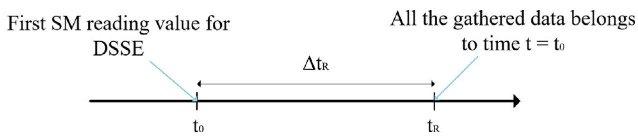

Fig. 3. DSSE is executed with timeliness of Δt_R.

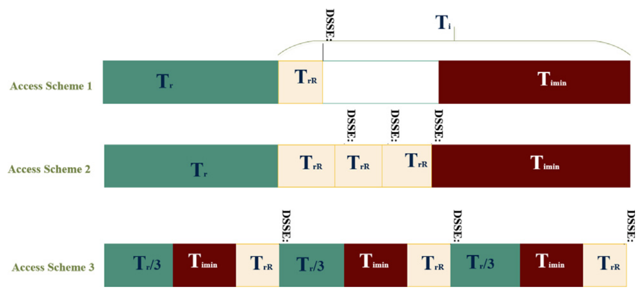

Fig. 4. AMI Access Schemes.

time interval centered on t_0). As a consequence, if the DSSE is executed using metering data with the timeliness of Δt_R seconds, the estimated states correspond to a time instant of Δt_R seconds in the past.

3.3. Access to smart meter data for state estimation

Fig. 4 shows three different access schemes, which define how the spare idle time is used for accessing selected SMs for state estimation. In that figure, T_{rR} refers to the time allocated for reading the selected SMs. The schemes differ in the execution frequency and in the spacing of the state estimation, in the maximum size of the time slot allocated for reading the selected SMs.

Access Scheme 1 leads to an execution of the state estimation with a constant period equalling the total reading time of the AMI. Advantage of the scheme is that it would allow for the largest number of SMs to be scheduled for selected access, as a single T_{rR} can fill out the maximum idle time. On the other hand, it results in a low execution frequency of the state estimation.

Access Scheme 2 provides the opportunity for accessing the state estimation multiple times per AMI cycle. Drawbacks are the resulting shorter intervals T_{rR} and the irregular spacing of the DSSE execution. *Access Scheme 3* reduces the disadvantage of the irregular spacing of the DSSE execution, at the price of breaking up the legacy reading cycle of all Smart Meters in several blocks - so requires a modification of the legacy process.

In this work we focus on one single idle time window regardless of the access scheme utilized. The analysis in Section 5 will be applicable to all three access schemes; only the parameter ranges will be different in terms of the maximum T_{rR} that is available between the schemes.

3.4. Grid topology scenario for assessment

Fig. 5 shows the reference grid scenario used for the study in the paper. The model is representative of a real rural LV grid in Denmark [5], and yet it is small enough to have a computationally feasible scenario. Due to the nature of rural areas, households are scattered in large geographical areas which contributes to a smaller number of customers connected by longer feeders. In this case, the total number of connected customers are 19, all of them equipped with a SM. Additionally, the secondary side of the substation is assumed to have a SM. Thus, the total number of SMs in the area is 20.

While it is straightforward also to add more distributed generation to this LV grid, the operating scenarios in the analysis performed in the next sections only consider consumption in order to delimit the parameter space.

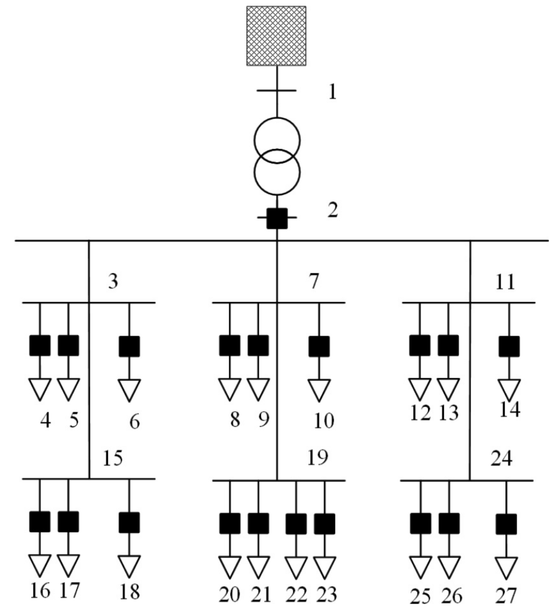

Fig. 5. LV Grid Scenario, the black squares represent the position of the 20 SMs.

4. Analysis of timeliness of access to selected SMs

As introduced in an earlier subsection, the timeliness of the SM measurements will depend on the number of SMs, R, that are accessed for DSSE during the time slot(s) of size T_{rR} within total AMI reading cycle. We start by first elaborating of this T_{rR} interval. A message sequence chart for a two-layer AMI data access system is shown in Fig. 6.

The presented two-layer architecture in Fig. 6 shows SMs at the bottom, which perform the local measurements of voltage magnitude, active power, and reactive power. The SMs forward the measurement taken around t_{0R} upon request by the data concentrator. D_1 represents the round-trip communication delay between SM and concentrator and is affected by the number of hops in the path between SM and

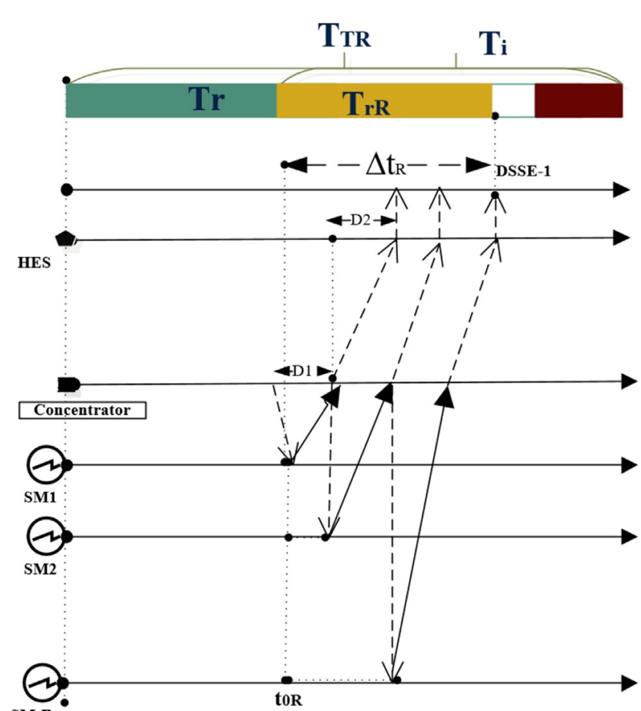

Fig. 6. Detailed procedures and timing for access to selected SMs for state estimation.

concentrator. D_2 is the delay between concentrator and the Head End System (HES). Timeliness Δt_R is the maximum time it takes to read R SMs with $\Delta t_R \leqslant T_{rR}$.

Measurements that are expected to be done at time t_{0R} such that the first meter can immediately reply to the initial response, are assumed to be locally planned and scheduled ahead of time. Behind the shown process, a clock synchronization protocol is ensuring a reasonable accurate clock synchronization between meters and thereby allows a synchronized measurement time point t_{0R} to be scheduled across the network. Each SMs will pick from the buffer and send the value from $t0R$.

The time difference between the snapshot measurements to the time that the state estimation application having all information available is analyzed as timeliness metric. Accessing data from R SMs in Fig. 6 affects the timeliness metric as the different SMs may have different path-lengths to the concentrator. To cope with the geographical spread of smart meters, we assume in our metering infrastructure, that a multi-hop meshed network is used. Each hop has a certain delay characteristic, and the total end-to-end delay consists of a sum of delays, depending on the amounts of hops between the concentrator and meter. Considering the constraint $T_{rR} < (T_i - T_{imin})$, and deterministic single hop communication delays, the resulting Δt_R value is:

$$\Delta t_R = D_1^{(1)}/2 + \sum_{n=2}^{R} (D_1^{(n)}) + D_2, \tag{1}$$

where $D_1^{(n)}$, $n = 1, \ldots, R$ is the round-trip time delay for the n-th accessed selected smart meter. When there are a different number of hops for the communication path to the selected Smart Meters, these roundtrip delays will vary substantially accordingly.

4.1. AMI cycle and communication parameters

To perform trade-off analysis between timeliness and the accuracy for LV DSSE, three different communication topologies are considered: (1) all Smart Meters are in single-hop distance to the concentrator; (2) all Smart Meters are in 5-hop distance to the concentrator; (3) is a heterogeneous case in which all path-lengths from 1-hop to 5-hop occur. This heterogeneous scenario is designed in such a way that the distribution of all path-lengths is constant, so 20% of the SMs are in distance from first to the fifth hop, respectively. In all scenarios, we consider that the 20 SMs shown in Fig. 5 are all connected to a single DC. We then vary the number of selected SMs from $R = 7$ to $R = 20$ in order to analyze the different resulting timeliness.

Due to the sequential request/response pattern, and thereby deterministic access to the medium, there is generally little interference between different smart meters. We therefore assume under otherwise good channel conditions, that delays are deterministic. Values for $D_1 = 10$ s and $D_2 = (1/4)$ s are motivated by RF mesh and 3G based networks at between SM and concentrator, and concentrator and headend, respectively [5]. Usually, these delays depend on the message sizes, and thus on the number of measurements to be transmitted, the assumption here is that the packets have fixed size leading to a constant delay. 1-hop and 5-hop scenarios represent best and worst AMI scenarios motivated by realistic AMI systems with meshed networks [5]. Table 1 summarizes the used parameters. An AMI cycle of $T_{TR} = 1$ h is used with an idle time $T_I = 24$ min.

Table 1
AMI cycle and communication parameters.

1-hop RTT SM-DC	DC-HE delay	T_{TR}	T_I
10 s	0.25s	1 h	24 min

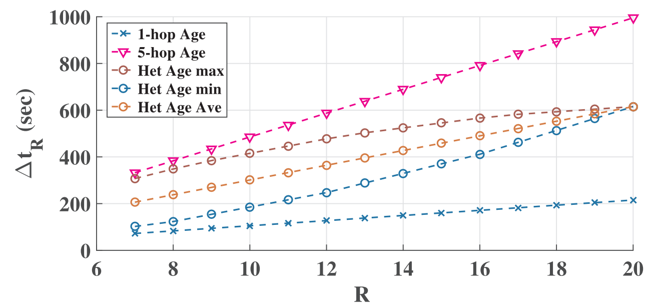

Fig. 7. Relationship between number of relevant SMs and the resulting Δt_R for the three communication topology scenarios. Maximum, minimum and average for the one- and five-hop scenarios are on top of each other, because of the deterministic delay, caused by the assumption of good channel conditions and the sequential access to the meters.

4.2. Impact of selected smart meters on timeliness

We investigate in this analysis the impact of different selections of the R Smart Meters on the timeliness by exploring all possible combinations of selecting R Smart Meters, and varying R in the range from $R = 7$ to $R = 20$. We consider in this analysis three different types of communication topologies as introduced in the previous subsection, representing different situations, (1) one where all meters are very close, i.e. 1-hop distance, to the concentrator, (2) one where all meters has to go through four other meters before reaching the concentrator; (3) a mixed case in which all path-lengths from 1 to 5 occur with approximately equal likelihood. The analysis targets to how does the number R of Smart Meters and the selection of specific SMs affect Δt_R.

Fig. 7 shows the relationship between the number of selected SMs, R, and timeliness Δt_R. Maximum and Minimum as well as average over the possible selection of R selected Smart Meters are shown, while these only lead to different values in the heterogeneous path-length case. For the 1-hop and 5-hop scenario, every selection of R SM gives the same Δt_R, we therefore only plot the average value of the two cases. The 5-hop values give higher Δt_R due to the added delay to transfer the message from SM to DC in multiple hops. Due to the assumption of deterministic delays, the behaviour for one and five hops is linear. Having 1-hop SMs naturally leads to the lowest timeliness as the maximum number of SMs we could accommodate is higher than for 5-hop scenarios.

To give an example for a given Δt_R, one can accommodate all the 20 first hop SMs, but only on average seven SM in a heterogeneous scenario. The heterogeneous case gives us a more realistic scenario where SMs are scattered in different hops. The analysis here is used later to discuss the trade-off between Δt_R and estimation accuracy.

Although a maximum of 1000 s. may appear fairly long to be considered real-time, an accurate state estimation of the low-voltage grid for some 15 min backwards in time still has high value for the DSO: In particular for fault management scenarios, i.e. fault detection and diagnosis applications, a 15 min response time is still a dramatic improvement compared to the current methods based on customer calls and manual search. Furthermore, note that the timeliness of the state estimation will improve when faster communication networks to the smart meters are implemented. So the assessment methodology and results of this paper can also be used to determine communication network requirements for future smart meter deployments.

5. Grid state estimation

In this part, we focus on the grid state estimation that is performed based on the data collected from the AMI.

5.1. Weighted least squared state estimation

In our paper we use a WLS algorithm that minimizes the function:

$$\text{minimize} J(x) = \sum_{i=1}^{m} \frac{(z_i - h(x))^2}{\Sigma_{ii}} \tag{2a}$$

$$\text{subjected to } z_i = (h(x))_i + \epsilon_i \tag{2b}$$

where z is the measurements vector, $h(x)$ is a vector of equations relating the states x with the measurement vector z, and Σ is the covariance matrix of measurement errors ϵ_i. If the errors between measurements are assumed to be independent, then Σ is a diagonal matrix. We define $W := \Sigma^{-1}$.

The measurement vector in the scenario of this paper consists of the voltage magnitudes, active power values, and reactive power values of the R selected Smart Meters at access time t_{0R}, so $3R$ real values. In addition, pseudo-measurements of active power and reactive power are used for the remaining $N - R$ customer Smart Meters that have not been selected for access, providing another $2(N - R)$ real valued components of the vector z. The generation of these pseudo-measurements will be explained later.

The minimal solution satisfies the first-order optimality conditions:

$$g(x) = \frac{J(x)}{\partial x} = -H^T(x)W\left[z - h(x)\right] = 0 \tag{3}$$

where $H(x) = \left[\frac{\partial h(x)}{\partial x}\right]$

Using Taylor series expansion to linearize $g(x)$ around the state vector x^k (neglecting higher order terms) yields:

$$g(x) = g(x^k) + G(x^k)(x - x^k) = 0 \tag{4}$$

The system above can be solved by the Gauss-Newton method in an iterative fashion:

$$\Delta x^{k+1} = G(x^k)^{-1}H(x^k)^T W[z - h(x^k)] \tag{5}$$

$G(x)$ is known as the gain matrix of the system and equals:

$$G(x^k) = H(x^k)^T W H(x^k) \tag{6}$$

The inverse of $G(\hat{x})$ is the covariance matrix of the estimated states [29]:

$$\hat{P} = (H(\hat{x})^T W H(\hat{x}))^{-1} \tag{7}$$

The measurement function $h(x)$ is composed of equations relating the input measurements with the actual state variables. The way these equations are formulated is dependent on the utilized grid model. For example, two-port π-model for the grid branches [4], three-phase feeder model as in [15], etc., and the chosen state variables, i.e., nodal voltages or branch currents in polar or rectangular form. In this paper, the WLS DSSE methodology presented in [15] is approached where the estimated states are the voltage phasors at every node of the system expressed in rectangular form.

5.2. Usage and interpretation of error covariance matrix

Consider the error covariance matrix as indicated in Eq. (7). As indicated in [29], since the measurement errors are assumed to be normally distributed a $\pm 3\sigma$ deviation around the mean covers approximately 99.73% of the Gaussian curve. Therefore, an approach to calculate the measurement weights is:

$$\sigma_{zi} = \frac{\mu_{zi}\cdot e}{3} \tag{8}$$

where $\pm e$ is the maximum measurement error relative to the measurement value.

Note that μ_{zi} is the actual measurement, and it depends on the system operating scenario and the Gaussian error added by the measurement device. Therefore, the error covariance matrix of the estimated states is only valid for the estimates obtained given a set of measurements. However, quantifying the variances of the estimated states considering multiple operating scenarios can be achieved by calculating the expectation of the state error covariance matrix based on a large set of Monte Carlo simulations of different load conditions of the grid:

$$P = E[\hat{P}], \tag{9}$$

which is used for evaluation in the upcoming sections. The diagonal of the covariance matrix gives the variances of the rectangular coordinates of the estimated states. Note that the largest of the diagonal entries in this matrix defines the estimated state with the worst accuracy, and thus this worst accuracy is used as metric in further analysis. Hereby, the substation MV and LV busbar are excluded, in order to investigate the improvement of accuracy on the junction boxes and customer nodes [30].

5.3. Measurements and pseudo-measurements

Pseudo-measurements of active and reactive power are assumed to be available for ALL customer smart meters: the values of the measurement of P and Q during the regular reading cycle (during the time period T_r) are used for these. The detailed model of the error of these pseudo-measurements will depend on access scheme as introduced in Section 3.3. This detailed analysis is out of scope of this paper; as the example uses a reading cycle time of 1 h (see Table 1), the error due to the age of these measurements is represented by a Gaussian random variable with a large standard deviation of 50% of the true value.

The measured values of the R selected smart meters at time t_{0R} are active and reactive power, with an added Gaussian measurement error of $\pm$ 3%; in addition these Smart Meters measure the voltage magnitude with a Gaussian error $\pm$ 1%[31]. All smart meter measurements are assumed to be a single real value (lumped over the three phases) measured by the Smart Meter over an interval of several seconds around t_{0R}. In practice, the DC will request the corresponding measurement value from the ring buffer of the Smart Meter device; the required clock synchronisation between the selected smart meter devices needs to be in the order of few seconds, which is achievable in most practical settings; see [32] for additional error quantification of de-synchronized clocks.

5.4. Simulation approach

In order to analyze the dependence of the accuracy of the DSSE for an increasing number of selected Smart Meters, R, initially, a set of $R = 7$ smart meters is selected as follows: The substation smart meter is included, and then from each junction box bus bar, one Smart Meter is randomly selected and added to the set. This results in the minimal number of $R = 7$ Smart Meters, as there are six junction box bus bars in the used topology. This initial selection is chosen, in order to assure a minimal observability of the LV grid.

After performing the calculation of the state estimator quality for a chosen number of R Smart Meters, the selected Smart Meter Set is increased by one randomly selected Smart Meter from the remaining $N - R$.

For each value of R, 1000 load scenarios are generated randomly, in which each of the 19 customer loads is sampled independently from a Gaussian distribution. For simplicity reasons, balanced loading scenarios are considered, i.e., same power consumption in each phase of a given customer. Operating scenarios have been created by changing the loading conditions accordingly in each customer as the input data to a load-flow algorithm as in [33] and implemented in Matlab. The outcome of the load-flow calculation are the assumed true voltage and current phasors in rectangular form. However, as input to the state

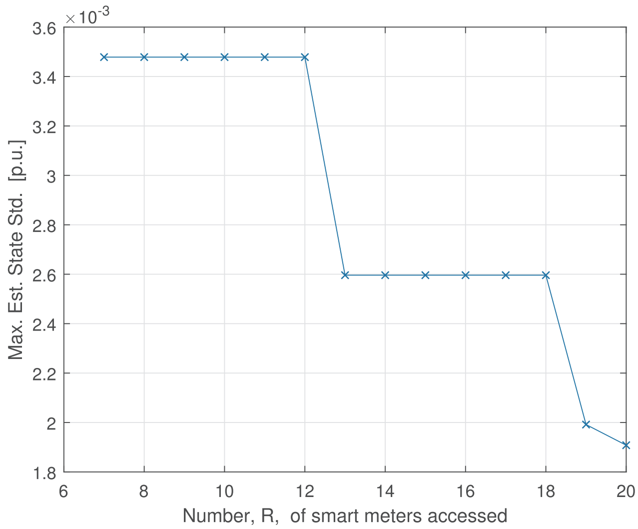

Fig. 8. Largest estimated state standard deviation, obtained from diagonal of state error covariance matrix (see Eq. (7)).

estimation, we use erroneous measurements by adding a Gaussian error, see previous subsection.

5.5. Analysis of DSSE accuracy based on available data

In order to analyze DSSE accuracy, we use the obtained expected value of the covariance matrix in Eq. (9), for which the expected value is obtained by calculation using the synthetically erroneous measurements from the simulated 1000 load scenarios. We furthermore introduce another accuracy metric, Root Mean Square Error (RMSE), below. From both accuracy metrics, variance respectively error values result for each grid location, calculated over the 1000 different load scenarios. We subsequently use the worst (largest) variance or RMSE value in order to represent the accuracy of the DSSE method as it provides an upper bound on the DSSE accuracy.

Fig. 8 shows the largest value of the square root of the state error covariance matrix diagonal entries, obtained when assuming that different number of relevant smart meters (R) are accessible in the dedicated access cycle during the idle time. Note that the accuracy measure on the y-axis (obtained from the state error covariance matrix) in Fig. 8, is given in per units, since the nodal voltages within the DSSE algorithm are calculated per unit.

The accuracy values obtained by this approach are shown in Fig. 8, which shows the largest observed state standard deviation obtained by the 1000 MC runs. The results validate the approach of evaluating estimates accuracy based on the expectation of the state error covariance matrices as introduced in Eq. (9). The trend on DSSE accuracy is that generally having more relevant SMs improves the estimation. accuracy, which is as expected. It should be mentioned that the flat behaviour between $R = 7$ to 12 and again from $R = 13$ to R = 18, is a result of our accuracy metric being defined by the worst value across all grid locations. This worst value is not always benefiting by the added measurement location in R. In other words, the worst estimate can be fairly insensitive to additional measurements, and then can require several added measurements to improve. Estimates at other grid locations will benefit from each additional measurement, and this highly depends on their grid location relative to the added measurement point.

In addition to the square root of the largest expected value of the diagonal of the covariance metric of the estimated states, the accuracy of the estimator is also evaluated by the Root Mean Square Error (RMSE) of the estimated voltage magnitudes in component i $|\hat{x}_i^{(n)}|$ compared to the true voltage magnitudes $|x_i^{(n)}|$:

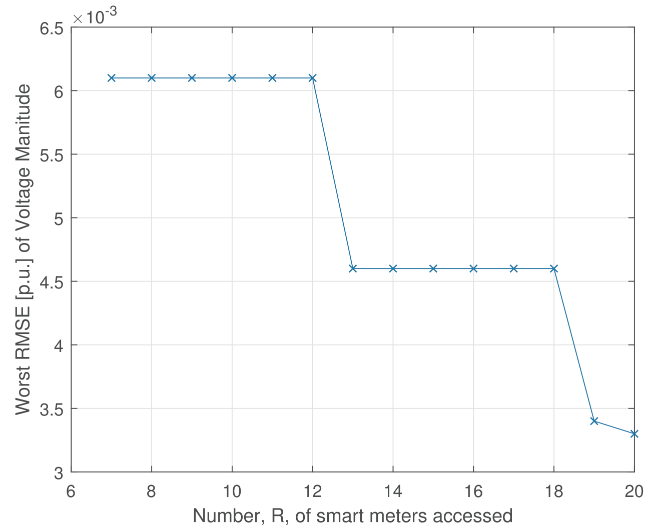

Fig. 9. Largest state RMSE (see Eq. (10)).

$$RMSE_{\hat{x}_i} = \sqrt{\frac{\sum_{n=1}^{N} (|\hat{x}_i^{(n)}| - |x_i^{(n)}|)^2}{N}} \tag{10}$$

The superscript thereby refers to the different load scenarios of the Monte Carlo simulation, i.e. the RMSE is taken per state over all node scenarios. In order to compare with the largest state covariance, the maximum (worst value) over all states i (corresponding to different grid locations) is then evaluated and plotted. The result of the RMSE metric is shown in Fig. 9; its qualitative behavior resembles Fig. 8.

Note that the horizontal behavior of both accuracy metrics between $R = 7...12$ and $R = 13...18$ results from the fact that the state with the largest variance determines the accuracy metric. The added Smart Meter measurement in these cases then does not help to improve this accuracy, because it was too far away in the grid topology. A targeted selection of an additional SM to improve specifically this state would lead to a better result - this optimized selection strategy will be investigated in future work. The observed insensitivity to added measurements of the estimates, thereby leads to the conclusion that as a selection criteria for smart meter measurement points in the access list, those near to the worst grid point that needs estimate must be prioritized. Note however, that the 'worst' grid location here in this paper is obtained by a large number of Monte Carlo simulations of different load scenarios. Therefore, it is not easy to in practice turn this into an online measurement device selection policy and that step will therefore be future work.

6. Assessment of trade-off between timeliness and DSSE accuracy

We now combine the analysis of the previous two sections, AMI timing analysis and grid state estimation accuracy in order to show the resulting trade-off quantitatively. The presented assessment approach enables to directly combine the results. This combined result is shown in Fig. 10. The results should be seen in the light that they generally depends on

- Followed criteria for SMs selection and prioritization which will be responsible for the accuracy improvement over the different sizes of vector R.
- AMI communication topology that is influencing the increase of timeliness while increasing the number of accessed SMs.

Here, the results are related to cases where additional smart meters are selected without further considerations to their strategic position in the grid.

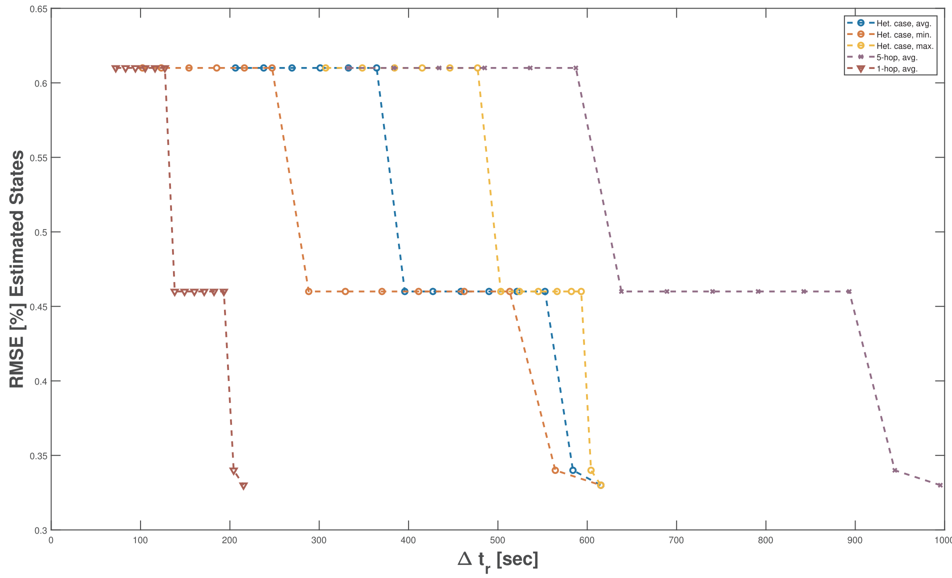

Fig. 10. Analysis of the relationship DSSE accuracy vs. timeliness for different sizes of vector R.

Plotting the key performance indicators as depicted before allows to easily decide the selection of SM data considering monitoring constraints defined by maximum allocated reading time T_{rR} for relevant SMs. The trade-off curves also provides knowledge on the expected accuracy of the estimates. For example, if the allocated T_{rR} bound is 400 s, it is easy to achieve good estimation accuracy for the one hop scenario. However, for the fifth hop scenario, with a similar T_{rR} bound of 400 s, it is hard to achieve a good accuracy, as the state estimation has to rely on only 8 of the 20 smart meters, and other measurements are replaced by the highly erroneous pseudo-measurements.

For the two cases 1 and 5 hops only, the max and min are not plotted, as they coincide with the average value. Hence there is only max and min values for the heterogeneous case shown in Fig. 10.

7. Conclusion and outlook

SMs in current LV distribution grids can be used to support LV distribution grid monitoring. Legacy SM reading cycles allocate idle times used for services such as firmware updates. Part of the idle time could be used to get measurements from selected SMs to support monitoring applications. However, due to the low bandwidth AMI communication technologies and a large amount of measuring points in LV grids, there are challenges to provide near real-time data access.

The concept of utilizing the spare idle periods for near real-time monitoring systems has been introduced in this paper and a methodology to asses the tradeoff between timeliness and state estimation accuracy has been presented. The methodology is applied to an example grid with 20 SMs for different realistic AMI communication topologies.

Future work includes the definition and assessment of intelligent selection of Smart Meters, the extension and application of the methodology to scenarios of stochastic communication delays, and the design of an adaptive data collection scheme for optimized access to SM data for distribution grid monitoring utilizing the tradeoff assessment methodology.

Declaration of Competing Interest

None.

acknowledgments

This work has been financially supported by the Danish project RemoteGRID which is a ForsKEL program under Energinet.dk with grant agreement No. 2016-1-12399 and by the European Union's Horizon 2020 research and innovation program under grant agreement No 774145 within the project Net2DG. The authors would like to thank all project partners for their feedback and input.

Appendix A. Supplementary material

Supplementary data associated with this article can be found, in the online version, at https://doi.org/10.1016/j.ijepes.2020.106090.

References

[1] Saint-Pierre A, Mancarella P. Active distribution system management: a dual-horizon scheduling framework for dso/tso interface under uncertainty. IEEE Trans Smart Grid 2017;8(5):2186–97.
[2] Pepermans G, Driesen J, Haeseldonck D, Belmans R, haeseleer W. Distributed generation: definition, benefits and issues. Energy Policy 2005;33(6):787–98.
[3] Stefan M, Lopez JG, Olsen RL. Exploring the potential of modern advanced metering infrastructure in low-voltage grid monitoring systems. In: 2018 IEEE international conference on big data (Big Data). IEEE; 2018. p. 3543–8.
[4] Gomez-Exposito A, Abur A. Power system state estimation: theory and implementation. CRC Press; 2004.
[5] Remotegrid. [Online]. Available: <http://www.remotegrid.dk/>.
[6] Schweppe FC, Wildes J. Power system static-state estimation, part I: exact model. IEEE Trans Power Appar Syst 1970;1:120–5.
[7] Wu H, et al. Pmu impact on state estimation reliability for improved grid security. 2005/2006 IEEE/PES transmission and distribution conference and exhibition. IEEE; 2006. p. 1349–51.
[8] Sanchez R, Iov F, Kemal M, Stefan M, Olsen R. Observability of low voltage grids: Actual dsos challenges and research questions. In: 2017 52nd international universities power engineering conference (UPEC). IEEE; 2017. pp. 1–6.
[9] Baran ME, Kelley AW. State estimation for real-time monitoring of distribution systems. IEEE Trans Power Syst 1994;9(3):1601–9.
[10] Baran ME, Kelley AW. A branch-current-based state estimation method for distribution systems. IEEE Trans Power Syst 1995;10(1):483–91.
[11] Teng J-H. Using voltage measurements to improve the results of branch-current-based state estimators for distribution systems. IEE Proc-Gener, Transmiss Distrib 2002;149(6):667–72.
[12] Li K. State estimation for power distribution system and measurement impacts. IEEE Trans Power Syst 1996;11(2):911–6.
[13] Meliopoulos AS, Zhang F. Multiphase power flow and state estimation for power distribution systems. IEEE Trans Power Syst 1996;11(2):939–46.
[14] Deng Y, He Y, Zhang B. A branch-estimation-based state estimation method for radial distribution systems. IEEE Trans power Deliv 2002;17(4):1057–62.
[15] Lu C, Teng J, Liu W-H. Distribution system state estimation. IEEE Trans Power Syst 1995;10(1):229–40.

[16] Lin WM, Teng JH. State estimation for distribution systems with zero-injection constraints. In: Proceedings of power industry computer applications conference. IEEE; 1995. p. 523–9.
[17] Baran M, McDermott T. Distribution system state estimation using ami data. In: 2009 IEEE/PES power systems conference and exposition. IEEE; 2009. p. 1–3.
[18] Wu J, He Y, Jenkins N. A robust state estimator for medium voltage distribution networks. IEEE Trans Power Syst 2012;28(2):1008–16.
[19] Liu J, Tang J, Ponci F, Monti A, Muscas C, Pegoraro PA. Trade-offs in pmu deployment for state estimation in active distribution grids. IEEE Trans Smart Grid 2012;3(2):915–24.
[20] Gómez-Expósito A, Gómez-Quiles C, Džafić I. State estimation in two time scales for smart distribution systems. IEEE Trans Smart Grid 2015;6(1):421–30.
[21] Asprou M, Kyriakides E. The effect of time-delayed measurements on a pmu-based state estimator. In: 2015 IEEE Eindhoven PowerTech. IEEE; 2015. pp. 1–6.
[22] Zhu K, Nordström L, Al-Hammouri AT. Examination of data delay and packet loss for wide-area monitoring and control systems. In: 2012 IEEE international energy conference and exhibition (ENERGYCON). IEEE; 2012. p. 927–34.
[23] Schwefel H-P, Rasmussen JG, Olsen RL, Ringgaard H, Silva N. Using smart meter measurements to manage accuracy of current calculations in lv feeders. In: IEEE Smartgridcom; 2019.
[24] Dehghanpour K, Wang Z, Wang J, Yuan Y, Bu F. A survey on state estimation techniques and challenges in smart distribution systems. IEEE Trans Smart Grid 2019;10(2):2312–22.
[25] Erlinghagen S, Lichtensteiger B, Markard J. Smart meter communication standards in Europe–a comparison. Renew Sustain Energy Rev 2015;43:1249–62.
[26] Findrik M, Groenbaek J, Olsen RL. Scheduling data access in smart grid networks utilizing context information. In: 2014 IEEE international conference on smart grid communications (SmartGridComm). IEEE; 2014. p. 302–7.
[27] Kemal MS, Olsen RL, Schwefel HP. Optimized scheduling of smart meter data access: a parametric study. In: 2018 IEEE international conference on communications, control, and computing technologies for smart grids (SmartGridComm). IEEE; 2018. p. 1–6.
[28] Angioni A, Schlösser T, Ponci F, Monti A. Impact of pseudo-measurements from new power profiles on state estimation in low-voltage grids. IEEE Trans Instrum Meas 2016;65(1):70–7.
[29] Singh R, Pal BC, Vinter RB. Measurement placement in distribution system state estimation. IEEE Trans Power Syst 2009;24(2):668–75.
[30] Asprou M, Kyriakides E. Optimal pmu placement for improving hybrid state estimator accuracy. In: 2011 IEEE Trondheim PowerTech. IEEE; 2011. p. 1–7.
[31] Pau M, Pegoraro PA, Sulis S. Efficient branch-current-based distribution system state estimation including synchronized measurements. IEEE Trans Instrum Meas 2013;62(9):2419–29.
[32] Schwefel HP, Antonios I, Lipsky L. Impact of time interval alignment on data quality in electricity grids. In: 2018 IEEE international conference on communications, control, and computing technologies for smart grids (SmartGridComm). IEEE; 2018. p. 1–7.
[33] Ciric RM, Feltrin AP, Ochoa LF. Power flow in four-wire distribution networks-general approach. IEEE Trans Power Syst 2003;18(4):1283–90.

Mohammed Kemal received his B.Sc degree in Electrical, Electronics and Communications Engineering from Jimma University, Ethiopia and M.Sc degree in Network and Distributed Systems from Aalborg University, Denmark in 2008 and 2014, respectively. From 2008 to 2012, he was working as a Telecom Engineer at Cresent Engineering and IT Solutions, Ethiopia. Where he was responsible for the design, installation, and monitoring of network and communication systems for multipurpose industrial infrastructures. In 2015, He has worked a Scientific Assistant at Department of Energy and Technology Aalborg University. Starting from 2016 he is pursuing his Ph.D. in the area of real-time monitoring of distribution grids using adaptive data collection of SM data at Department of Electronics of Aalborg University, Denmark.

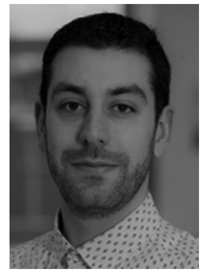

Ruben Sanchez received his B.Sc degree in Industrial Technical Engineering, specialization in Industrial Electronics from Alcala University, Spain and M.Sc degree in Power Electronics and Drives from Aalborg University, Denmark in 2014 and 2016, respectively. Starting from 2016 he is pursuing his Ph.D. in the area of real-time monitoring of low voltage distribution grids using smart metering data at Department of Energy Technology of Aalborg University, Denmark.

Rasmus L?venstein Olsen is an Associate Professor at Aalborg University working in the Wireless Communication Networks (WCN) group. Rasmus received his master degree from Aalborg University in 2003 and has received his PhD degree on the topic of Context Sensitive Service Discovery and Context Management with focus on access to dynamic information in 2008. Rasmus' current research focus is on the role of communication networks in smart grid and the impact of networks on remote access to dynamic data of the collection as well as the distribution of information. He is a member of several IEEE technical program committee and is currently active in the electrical association of Intelligent Energy in Denmark and been local chair for SmartGridComm 2018. He is currently engaged in national and European research smart grid projects; Net2DG, and WP leader in EU FP7 SmartC2Net on Experimental Prototypes. Rasmus is currently technical coordinator of the ForskEL (Energinet.dk) smart grid project RemoteGRID.

Florin Iov(S '98, M '04, SM '06) received the Dipl. Eng. degree in electrical engineering from Brasov University, Romania, in 1993 and a PhD degree from Galati University, Romania in 2003 with a special focus in the modeling, simulation and control of large wind turbines. He was staff member at Galati University, Romania from 1993 to 2001. Dr. Iov was with Institute of Energy Technology, Aalborg University, Denmark between 2001 and 2009 where he was mainly involved in research projects regarding wind turbines and wind power systems. From 2010 to 2012 he held a position as Power System Research Specialist in VestasWind Systems working with new ancillary services for augmented wind power plants. Since 2013 Dr. Iov is with Institute of Energy Technology focusing on research within smart grids.

Hans-Peter Schwefelis Professor for Communication Networks at Aalborg University, Denmark, and managing director of the startup company GridData (www.gridda-ta.eu). In parallel to his position at Aalborg University, he has previoulsy been Scientific Director of the Research Center for Telecommunications (Forschungszentrum Telekommunikation Wien - FTW) in Vienna, Austria in 2008–2016. His research focuses on IPbased communication networks and their applications for critical infrastructures with main interest in performance and dependability aspects. Before he joined Aalborg University, he was a project manager at Siemens Information and Communication Mobile, supervising research projects and responsible for the development of technical concepts for next generation mobile networks. He obtained his doctoral degree in the area of IP traffic and performance modeling from the Technical University in Munich, Germany.